



HAL
open science

A case study on the effects of foam and seat pan inclination on the deformation of seated buttocks using MRI

Xuguang Wang, Léo Savonnet, Loïc Capbern, Sonia Duprey

► **To cite this version:**

Xuguang Wang, Léo Savonnet, Loïc Capbern, Sonia Duprey. A case study on the effects of foam and seat pan inclination on the deformation of seated buttocks using MRI. *IISE transactions on occupational ergonomics and human factors*, 2021, 9, p 23-32. <10.1080/24725838.2021.1984340>. <hal-03380365>

HAL Id: hal-03380365

<https://hal.science/hal-03380365v1>

Submitted on 15 Oct 2021

HAL is a multi-disciplinary open access archive for the deposit and dissemination of scientific research documents, whether they are published or not. The documents may come from teaching and research institutions in France or abroad, or from public or private research centers.

L'archive ouverte pluridisciplinaire **HAL**, est destinée au dépôt et à la diffusion de documents scientifiques de niveau recherche, publiés ou non, émanant des établissements d'enseignement et de recherche français ou étrangers, des laboratoires publics ou privés.



HAL Authorization

1 **Title Page**

2

3 A case study on the effects of foam and seat pan inclination on the deformation of seated
4 buttocks using MRI

5

6 Xuguang WANG (corresponding author)

7 Research Director

8 LBMC/TS2

9 Université Gustave Eiffel

10 Email address: xuguang.wang@univ-eiffel.fr

11

12 Léo Savonnet

13 Post-doctoral Researcher

14 LBMC/TS2

15 Université Gustave Eiffel

16 Email address: savonnet.leo@gmail.com

17

18 Loïc Capbern

19 Master student

20 LBMC/TS2

21 Université Gustave Eiffel

22

23 Sonia Duprey

24 Associate Professor

25 Université Lyon 1

26 sonia.duprey@univ-lyon1.fr

27

28

29

30

31 *Conflict of Interest (several sample statements are provided below)*

32 The authors declare no conflict of interest.

33

34 *Acknowledgments:*

35 The authors thank Andréa Gavard for her participation in data processing and Richard
36 Roussillon for his assistance in conception and building the mock-up used in the experiment
37 and the European Scanning Center for MRI scanning.

38

39 *Funding:*

40 The work is partly supported by Direction Générale de l'Aviation Civile (project n°2014 930818).

41

42

43

44

45

46 **Manuscript**

47

48 A case study of the effects of foam and seat pan inclination on the deformation of seated
49 buttocks measured using MRI

50

51 **Occupational Applications**

52 We investigated the effects of seat pan inclination and foam on the deformation of the seated
53 buttocks using an upright MRI system. From observations among four healthy males, we found
54 that soft tissue deformation under the ischial tuberosity (IT) could be reduced not only by using
55 a soft cushion, but also by decreasing the shear force on the seat pan surface. These results
56 suggest that soft tissue deformation could be used as an objective measure for assessing
57 seating discomfort and injury risk, by accounting for the effects of both contact pressure and
58 shear. We also confirmed that the gluteus maximus (GM) muscle displaced away from the IT
59 once seated. As peak pressure and shear are most likely located below the IT, more realistic
60 computational human body models in this region are needed that consider muscle sliding.

61

62 **Technical Abstract**

63 Background: A full understanding of soft tissue deformations, particularly in the gluteal region in
64 a seated position, would be helpful for improving seat comfort and reducing the injury risk of
65 seated people. Thanks to recent developments in medical imaging, direct observations of soft-
66 tissue deformations under realistic loading conditions is now possible using open MRI.

67 Purpose: The purpose of this work was to investigate the effects of seat pan inclination and
68 foam on the deformation of soft tissues in the gluteal region using an open MRI.

69 Methods: Four healthy male participants completed the experiment, in which a positional MRI
70 scanner was used to scan the buttocks and part of the thighs. Three seating conditions were
71 tested by varying the seat pan angle (A_{SP}) and cushion material while the backrest was fixed

72 at 22 degrees from the vertical: 1) A_SP=7° without foam (Reference); 2) A_SP=0° without
73 foam (Shear); 3) A_SP=7° with a 50 mm thick foam on the seat pan (Foam). In addition, one
74 configuration (Unloaded), with the buttocks being unsupported, was also scanned for
75 comparison. After segmenting images, we calculated the volumes of the gluteus maximus (GM)
76 muscle and subcutaneous fat in three regions of interest under the ischial tuberosity (IT) for
77 each condition.

78 Results: Once seated, the GM displaced away from the IT laterally and posteriorly. For all
79 participants, the largest tissue deformation was observed in the Shear condition, while the
80 smallest was found in the Foam condition.

81 Conclusions: The present study provides quantitative data needed for validating buttock-thigh
82 finite element models. Future work is needed to link soft tissue deformation with discomfort
83 perception.

84

85 **Keywords:** Seating, Comfort/discomfort, soft tissue, deformation, biomechanics, MRI, Finite
86 element modeling

87

88 1 Introduction

89 People spend more and more time seated in transportation, at home, and at an office. Comfort
90 is not only an important sales argument for the seat manufacturers, but is also well recognized
91 as an important health factor for sitters. Long-term sitting may lead to discomfort (De Looze et
92 al., 2013, Hiemstra-van Mastrigt et al., 2017), and even to pressure sores for wheelchair users
93 (Olesen et al., 2010). Despite the large number of existing seating (dis)comfort studies, there is
94 a lack of objective methods for assessing seating discomfort. De Looze et al. (2003) proposed a
95 conceptual model of seating comfort and discomfort based on a literature review. They
96 suggested that stronger relationships with objective measures might exist for discomfort
97 compared to comfort, in agreement with the model of comfort and discomfort initially proposed
98 by Zhang et al. (1996). Among the 21 studies reviewed by De Looze et al., the following
99 objective measures were used: sitting posture and movement shifts, muscle activities measured
100 by EMG, pressure distribution, spinal load indirectly estimated by stature loss, and foot swelling.

101 Thanks to its ease of use and relatively low cost, a pressure mapping system is
102 frequently used for objectively assessing seating discomfort. Zemp et al. (2015) reviewed
103 studies investigating the relationships between pressure and discomfort. They concluded that
104 the question whether contact pressure measurements are suitable for assessing seating
105 comfort or discomfort could not yet be answered definitely, due to limited available data. More
106 recently, Hiemstra-van Mastrigt (2017) made an extensive review on passenger seat comfort
107 and discomfort in a human-product-context interaction. They found that there exist correlations
108 between anthropometric variables and interface pressure variables, and that these relationships
109 are posture dependent. However, the relationships between pressure variables and passenger
110 comfort and discomfort are still not clear and could not be quantified due to a lack of statistical
111 evidence.

112 Apart from interface pressure, other biomechanical parameters such as intervertebral
113 disc pressure, soft tissue deformation, muscle forces, shear force at contact interface, are rarely
114 studied, even though they are generally considered as relevant for assessing seating discomfort
115 (see for example, Rasmussen et al., 2009 and Al-dirini et al., 2015). In particular, high shear
116 forces on the seat may lead to large deformations of soft tissues and reduced blood flow
117 (Goossens et al., 1994). The main reason for this lack of studies is that these biomechanical
118 parameters cannot be easily measured experimentally. Computational human models are
119 therefore needed to estimate these biomechanical variables indirectly. Two types of human
120 models have been developed, deformable finite element (FE; see Savonnet et al., 2018 for a
121 review) and rigid multi-body musculoskeletal (MSK; Rasmusen et al., 2009) models. However,
122 these models are generally not validated under the conditions relevant for seating applications
123 (Wang et al., 2019b).

124 Most existing studies on seating comfort used a real seat or an experimental seat
125 affording little opportunity to vary design parameters (Hiemstra-van Mastrigt et al., 2017). It is
126 therefore difficult to isolate the effects of a particular seat parameter or to examine interactions
127 with other variables. To understand the effects of shear force, and to develop quantitative
128 guidance regarding seat design, we recently built a multi-adjustable experimental seat equipped
129 with force sensors to measure all contact forces (Beurier et al., 2017). We investigated the
130 effects of seat parameters and anthropometric dimensions on preferred seat profile and contact
131 forces (Wang et al., 2018 and 2019a). Results of this work have provided quantitative guidelines
132 for the ergonomic design of future seats as well as data for validating computational human
133 models, especially for providing loading boundary conditions. Further, we used both deformable
134 FE (Savonnet, 2018) and MSK (Theodorakos et al., 2018) modeling approaches for assessing
135 seating discomfort. Thanks to recent progress in medical imaging, it is possible to observe spine
136 and pelvis positions and soft tissue deformation directly. Existing computational human models
137 need to be further validated with the help of medical images in seating conditions and with

138 realistic boundary conditions. Relationships between biomechanical parameters and discomfort
139 still need to be further investigated, so that objective criteria could be defined and implemented
140 in a computerized human model.

141 In recent years, a few researchers have used an upright MRI system to investigate soft
142 tissue anatomy in the buttocks during sitting, and have quantified soft tissue deformation
143 particularly in the ischial region (Al-Dirini et al., 2015, Sonenblum et al., 2015, 2018, 2020; Call
144 et al., 2017, Brienza et al., 2018). All of these studies, though, only focused on a single upright-
145 seated position, and most of them studied the effects of wheelchair cushion types on tissue
146 deformation. To our knowledge, few researchers have investigated the effects of seat design
147 parameters and their possible interaction on tissue deformation. Thus, the main objective of the
148 present work was to investigate, through a case study, the effects of seat pan inclination and
149 foam (indirectly contact pressure and shear force) on the deformation of soft tissues in the
150 gluteal region using an open MRI.

151 2 Methods

152 2.1 Participants

153 As a case study, four healthy male participants were recruited, and their characteristics are
154 summarized in Table 1. The ethics committee at the Université Gustave Eiffel's (formerly the
155 French Institute of Science and Technology for Transport, Development and Networks –
156 IFSTTAR) approved the experimental protocol. Informed consent was obtained prior to the
157 experiment for all participants. As the MRI system had a width of 60 cm in the scanning space,
158 participants were selected with a relatively small BMI, which varied from 20.3 to 27.6 kg/m².
159 None of the participants had metallic implants or suffered from claustrophobia.

160

161

162

163 **Table 1. Age, stature, body mass, and BMI of the four participants**

Participant	P1	P2	P3	P4
Age (years)	28	52	35	31
Stature (cm)	173	163	169	187
Body mass (kg)	61.2	67.3	77.6	79.8
BMI (kg/m ²)	20.3	25.9	27.6	23.6

164

165 2.2 Experimental conditions

166 While in an upright MRI scanner (Paramed® 0.5 Tesla, Figure 1), participants were scanned in
167 three seated positions and in one so-called ‘Unloaded’ position (Figure 2). The resolution of the
168 scans was set to 3.1 mm slice thickness, and 3.1 mm slice gap. The field of view was adjusted
169 to 300 x 300 x 150 mm in the sagittal, transversal, and coronal planes, respectively, for the left
170 side for each acquisition. For the Unloaded condition, the buttocks and thighs were free of
171 loading except gravity. The three seated conditions were defined by varying the seat pan angle
172 (A_SP) and cushion material, while the back was fixed at 22 degrees from the vertical: 1)
173 A_SP=7° without foam (Reference); 2) A_SP=0° without foam (Shear); and 3) A_SP=7° with a
174 50 mm thick foam on the seat pan (Foam).

175 The Reference configuration was defined based on our findings on the preferred seat
176 pan angle for a given back angle using a reconfigurable experimental seat (Wang et al., 2018).
177 We observed that people preferred a seat pan angle of about 7° for a back profile angle of 22°.
178 In addition, we observed that reclining the seat pan angle by 7° reduced the shear force on the
179 seat pan surface, by about 5% of body weight compared to sitting on a horizontal seat pan
180 (Wang et al., 2019a). We thus selected a horizontal seat pan for the Shear condition, which
181 could be considered more uncomfortable than the Reference condition. The last seating
182 configuration was the same as the Reference in terms of seat pan and back angles, except that
183 a foam of 50 mm thickness was added. Compared to the Reference, this ‘Foam’ condition was
184 expected to have a more uniform pressure distribution and a lower peak pressure under the
185 ischial tuberosities (ITs).

186 The seat pan and backrest were made of two wooden plates. The seat pan surface was
187 390 (length) x 500 (width) mm. We used a set of plates of different thicknesses to adjust the
188 seat height so that participants could sit comfortably. We verified that the frontal parts of the
189 thighs were just in contact with the seat pan. Compared to the Reference, the Shear condition
190 should have a shear force on the seat pan surface of about 5% of body weight higher (Wang et
191 al., 2019a). The force applied on the seat pan surface was verified after MRI scanning for the
192 participants. They were asked to reproduce the Reference and Shear positions, out of the MRI
193 scanning room, using our experimental seat equipped with force sensors for measuring contact
194 forces (Table 2). For the Foam condition, foam of 50 mm thickness fully covered the seat pan
195 plate. The foam was selected from those currently used for aircraft passenger seats.
196 Compression tests were conducted for the foam with a sample of 5 x 5 x 7cm³ using an Instron
197 mechanical test machine. Quasi-static compression loading and unloading were performed
198 (Figure 3).

199 For the Unloaded condition, we built a specific device providing supports for the arms,
200 back, knees, and feet, so that participants could easily keep the desired posture with the
201 buttocks and thighs being unsupported (Figure 2). The backrest was reclined 50° from the
202 vertical to bear most of the body weight. We controlled the back-thigh angle (about 105°) by a
203 goniometer, close to the Reference condition. The Unloaded condition was tested first, followed
204 by the Reference, Foam, and Shear conditions.

205 Because of the limited scanning volume, we had to carry out two acquisition sequences
206 to cover the buttocks and part of the thighs. A pre-imaging step was performed before each
207 acquisition to ensure that the two windows of imaging overlapped, based on markers placed on
208 the skin. Each acquisition sequence took about 8 minutes, during which participants were asked
209 to remain immobile.

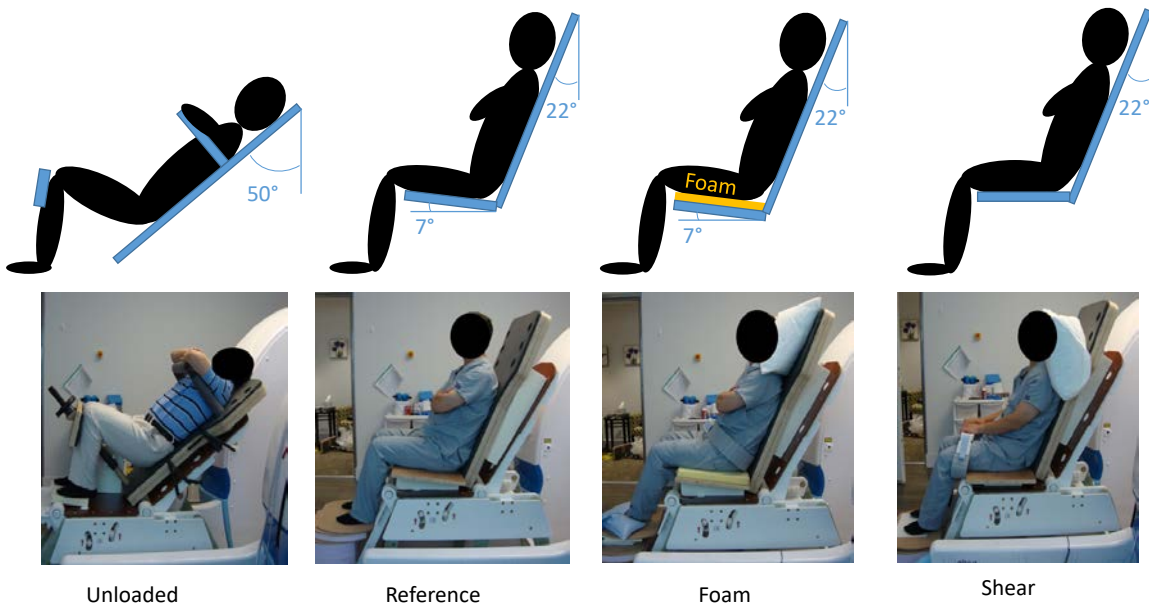
210



211
212
213

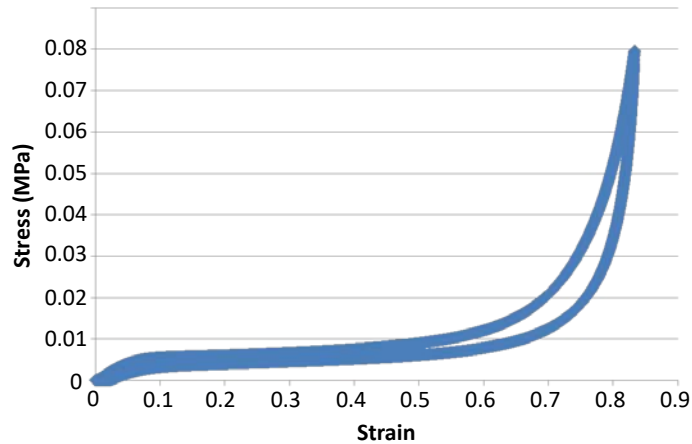
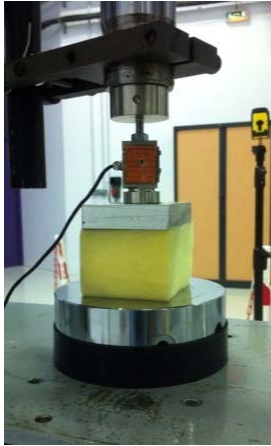
Figure 1. An overview of a participant undergoing the MRI imaging protocol

214



215
216
217

Figure 2. Illustration of the four testing conditions in the upright MRI scanner environment.



219
220
221

Figure 3. Foam compression testing scenario (left) and stress-strain curve (right).

222
223
224
225

Table 2. Means (standard deviations) of the shear (negative forward) and normal (negative downward) components of the forces applied on the seat pan surface in the Reference and Shear seating conditions. Measurements were repeated three times for each condition.

Participant	Shear (N)		Normal (N)	
	Reference	Shear	Reference	Shear
P1	-19.2(4.3)	-52.7(7.8)	-445.4(10.0)	-443.3(7.0)
P2	-54.4(5.5)	-76.6(4.1)	-492.6(18.0)	-469.8(2.2)
P3	-75.6(8.3)	-118.6(7.8)	-550.2(40.2)	-562.8(4.1)
P4	-74.7(4.3)	-116.2(0.4)	-545.4(5.6)	-535.8(5.2)
All	-57.2(24.6)	-88.3(30.4)	-511.7(49.1)	-500(53.3)

226

227 2.3 Data processing and analysis

228 Raw DICOM data (Digital Imaging and Communications in Medicine, the standard for the
229 communication and management of medical imaging information and related data) were
230 imported into the open source software 3D Slicer (www.slicer.org) for manually segmenting the
231 pelvis, femur, gluteus maximus, and subcutaneous fat. Once segmented, 3D objects from the
232 two scans were exported in the MRI RAS coordinate system (X = right, Y = anterior, and Z =
233 superior). Objects were merged mainly by aligning the common part of the pelvis while ensuring
234 continuity of the skin envelope in contact with the seat, and re-meshed using the open source
235 software Meshlab (<https://www.meshlab.net/>). We defined three regions of interest (ROIs) using
236 three cylinders with diameters of 50, 20, and 10 mm. These cylinders were similar to those

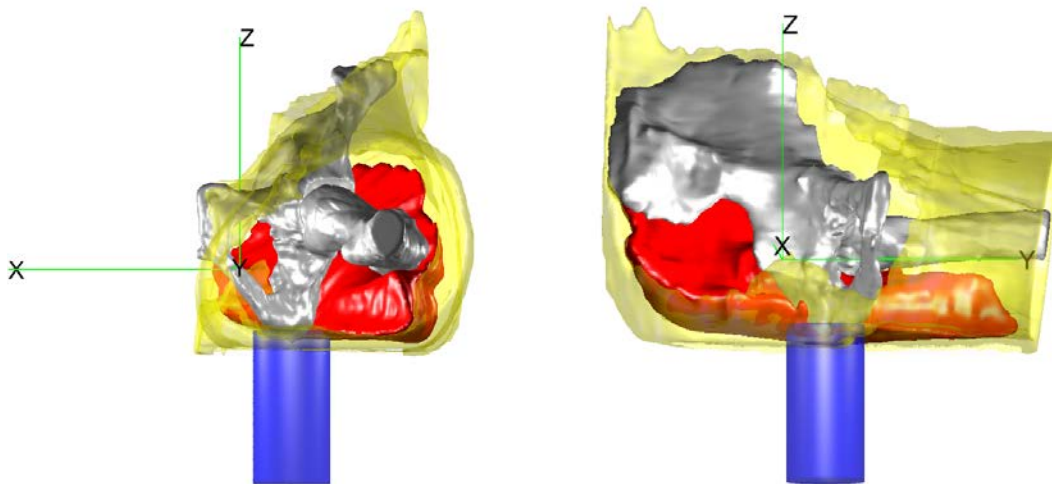
237 proposed by Sonenblum et al. (2015), who argued that the size of the IT is approximately 50
238 mm long and antero-laterally orientated. We also defined two ROIs with smaller diameters (10
239 and 20 mm) for a better focus on the region underneath the ITs. For the three seating positions,
240 the cylinders were perpendicular to the seat pan hard surface and centered at the ischium point
241 closest to the seat (Figure 4). Compared to the horizontal (x-y) plane in the MRI coordinate
242 system, the seat pan surface had respective angles of 7° and 0° in the Reference (also for
243 Foam) and Shear conditions (Figure 2). The cylinders were positioned such that the external
244 circle of the upper surface was in contact with the ischium. For the Unloaded condition, which
245 had no seat pan, the same ROIs as for Reference were used by aligning the pelvis. Volumes
246 and mean thicknesses of the bone, gluteal muscle, fat, and other tissues inside the ROIs were
247 calculated using a custom Matlab (R2020b) tool.

248 To quantify tissue deformation, we calculated tissue volume reduction in a ROI under the
249 IT in the three seated conditions with respect to the Unloaded condition, similar to the
250 approaches used by Brienza et al. (2018) and Sonenblum et al. (2015, 2018):

251

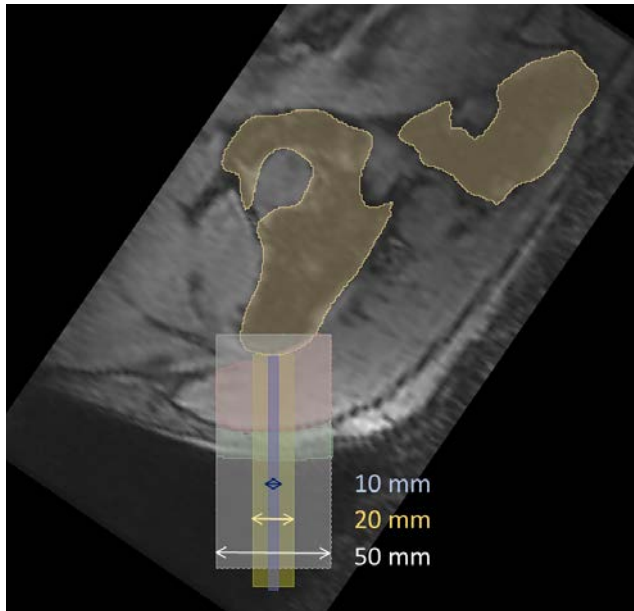
252 Tissue Volume Reduction (R) = $\left(1 - \frac{Tissue\ Volume_{loaded}}{Tissue\ Volume_{unloaded}}\right) \times 100\%$

253



254

255 (a)
256



257 (b)
258

259 **Figure 4. (a) Region of interest (ROI) characterized by a cylinder, illustrated for 50mm ROI of Participant #1 in**
260 **the Reference sitting condition. Three cylinders of 100 mm in length and 50, 20, and 10 mm in diameter were**
261 **used. Cylinder axes were perpendicular to the seat pan surface and centered at the ischium point closest to**
262 **the seat. Cylinders were positioned so that the external circle of the upper surface was in contact with the**
263 **ischium. (b) Three ROI illustrated with an MRI image in the sagittal plane for the Unloaded condition.**

264 3 Results

265 The four participants had quite different compositions of soft tissues in the ROI as shown in
266 results from the Unloaded condition (Table 3). Mean bulk tissue thicknesses in the 50 mm ROI
267 were 49.3, 61.2, 48.0, and 46.5 mm, and the percentages of the gluteus maximus (GM) muscle
268 were 55.1, 13.4, 8.4, and 27.1% respectively for participants P1 to P4. For the two narrower
269 ROIs (20 and 10 mm), P2 and P3 had almost no GM below the IT.

270 In the three-seated positions (Table 4), mean bulk tissue thicknesses in the 50mm ROI
271 were reduced to 18.9, 17.3, and 16.1 mm on average across participants in the Foam,
272 Reference, and Shear conditions, respectively, representing reductions of tissue volume (R) of
273 62.4, 65.5, and 68.1% with respect to the Unloaded condition. The Shear condition had the
274 highest deformation, followed by the Reference and Foam condition. These differences were
275 particularly obvious for the 10 and 20 mm ROIs below the IT (see Figure 5 for 10mm ROI). The

276 same trend was observed for all participants. Moreover, no GM was wrapped around the IT in
 277 the 10 and 20 mm ROIs once seated, even for P1 and P4, who each had an appreciable
 278 amount of the IT covered by the GM in the Unloaded condition. By visualizing the displacement
 279 of the GM from both 3D reconstructions (Figure S1 in Supplemental materials) and segmented
 280 MRI images (Figure S2 in Supplemental materials), it appears that the GM moved laterally and
 281 posteriorly.

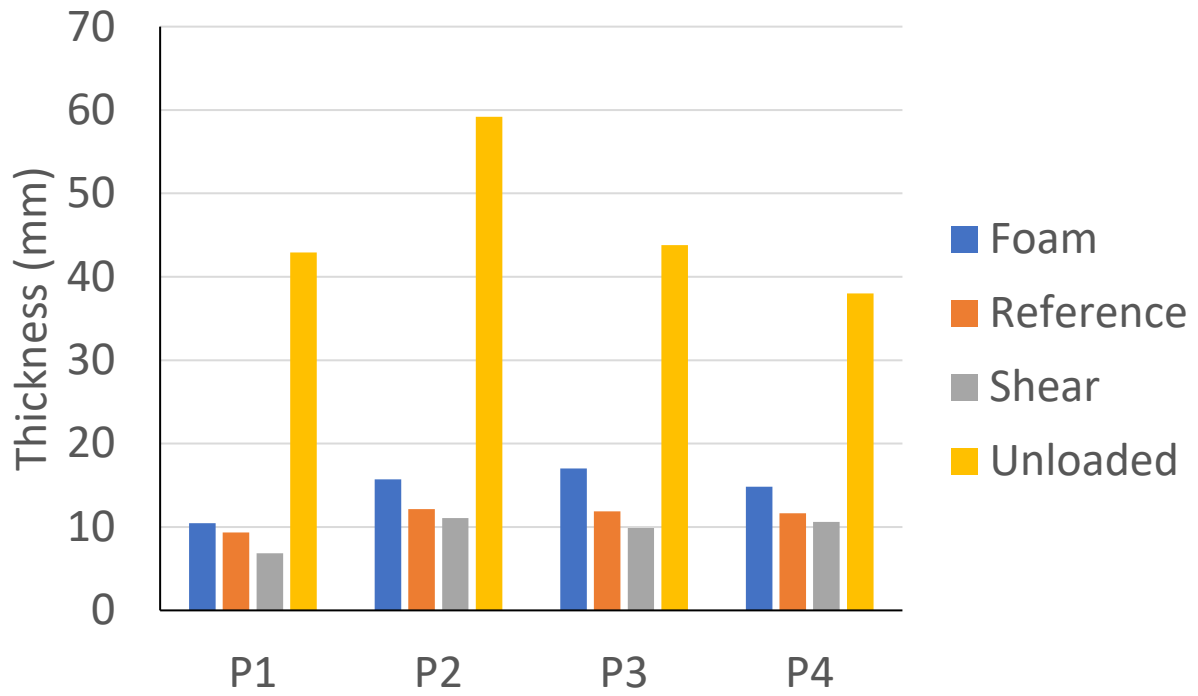
282

283 **Table 3. Volume and mean thickness of bulk tissue (T_tissue) under the ischium in the three ROI as well as**
 284 **the percentages of fat tissue, gluteus maximus muscle (GM), and other tissues in the Unloaded condition**

Participant	ROI	Bulk tissue volume (mm ³)	T_tissue (mm)	Fat (%)	GM (%)	Others (%)
P1	50	96728.3	49.3	32.9	57.4	9.7
	20	13769.7	43.8	27.6	71.4	1.0
	10	3371.9	42.9	28.0	72.8	-0.8
P2	50	120060.4	61.2	64.6	13.5	21.9
	20	18786.6	59.8	68.4	4.3	27.3
	10	4647.4	59.2	68.8	0.2	31.0
P3	50	94179.4	48.0	71.8	8.6	19.6
	20	13979.3	44.5	88.0	0.0	12.0
	10	3440.0	43.8	83.8	0.0	16.2
P4	50	91224.1	46.5	46.1	28.8	25.1
	20	12326.9	39.2	40.8	33.8	25.4
	10	2985.5	38.0	39.6	37.2	23.2
All	50	100548.0	51.2	53.8	27.1	19.1
	20	14715.6	46.8	56.2	27.4	16.4
	10	3611.2	46.0	55.0	27.5	17.4

285

286



287

288 **Figure 5. Mean bulk thickness under the ischium in the 10 mm ROI for the four test conditions**

289

290

291 **Table 4. Mean thickness of the bulk tissue (T_tissue) under the IT in the three ROIs as well as percentages of fat tissue, gluteus maximus muscle (GM),**
 292 **and tissue volume reduction (R in %) for the three seating conditions.**

293

Participant	ROI	T_tissue (mm)	Foam			T_tissue (mm)	Reference			T_tissue (mm)	Shear		
			Fat (%)	GM (%)	R (%)		Fat (%)	GM (%)	R (%)		Fat (%)	GM (%)	R (%)
P1	50	15.5	64.2	15.1	68.5	13.9	68.2	10.7	71.8	14.8	60.9	6.4	69.9
	20	11.1	73.6	0.0	74.7	11.3	71.3	0.0	74.3	7.7	72.2	0.0	82.3
	10	10.5	69.1	0.0	75.6	9.3	75.0	0.0	78.3	6.8	79.7	0.0	84.1
P2	50	18.6	51.2	0.0	69.6	15.6	56.3	0.0	74.4	15.2	52.4	0.1	75.1
	20	15.6	43.9	0.0	73.8	12.8	45.0	0.0	78.6	12.1	38.7	0.0	79.8
	10	15.7	42.1	0.0	73.4	12.1	48.7	0.0	79.5	11.1	37.7	0.0	81.3
P3	50	20.5	60.3	5.0	57.3	19.6	61.6	0.0	59.2	15.8	66.8	3.7	67.0
	20	16.6	64.3	0.0	62.7	12.8	48.8	0.0	71.2	10.7	60.2	0.0	76.0
	10	17.0	63.5	0.0	61.2	11.9	51.7	0.0	72.9	9.9	55.8	0.0	77.4
P4	50	21.0	52.3	6.2	54.8	20.3	55.9	0.0	56.4	18.5	67.5	0.8	60.2
	20	15.6	52.3	0.0	60.2	12.6	45.3	0.0	68.0	11.2	71.9	0.0	71.4
	10	14.8	54.0	0.0	61.0	11.6	44.3	0.0	69.4	10.6	71.6	0.0	72.1
All	50	18.9	57.0	6.6	62.4	17.3	60.5	2.7	65.5	16.1	61.9	2.7	68.1
	20	14.7	58.5	0.0	67.9	12.4	52.6	0.0	73.0	10.4	60.7	0.0	77.4
	10	14.5	57.2	0.0	67.8	11.2	54.9	0.0	75.0	9.6	61.2	0.0	78.7

294

295

296

297 4 Discussion

298 4.1 Summary of main observations

299 The present work aimed to investigate how seating condition affects soft tissue deformation
300 under the IT using an upright MRI system. The largest tissue deformation was observed in the
301 Shear condition, while the smallest was found in the Foam condition among all participants.
302 Though these findings were expected, to our knowledge, this is the first time that the effect of
303 shear force on tissue deformation was quantified directly. Compared to the Reference condition
304 with a seat pan angle of 7°, the Shear condition had a horizontal seat pan with the same
305 backrest inclination. Reducing the seat pan angle to 0° resulted in a forward shear force of 31 N
306 higher on average (an increase of 54.4% over 57.1N) (Table 2), while the force normal to the
307 seat pan surface was slightly affected proportionally (a difference of 12 over 512 N on average).
308 As peak pressure and peak shear stress are likely to be located under the IT, our results show
309 that a higher shear led to a higher soft tissue deformation. Of course, reducing peak pressure
310 using a soft cushion could also lead to a smaller tissue deformation as observed in the Foam
311 condition.

312 4.2 Comparison with past studies

313 Due to the differences in the methods used for defining the regions of interest (ROIs) as well as
314 in the experimental conditions, it is difficult to compare the results directly between different
315 studies. Our study is the first investigating the effects of both seat pan angle and cushion, while
316 all others kept the same seat pan inclination. We used the vertical cylinders of different
317 diameters with their axes being perpendicular to the seat pan surface as ROIs, similar to the two
318 cylindrical ROIs of 50 and 10mm defined by Sonenblum et al. (2015). In other words, the ROIs
319 in the present work were not fixed to the pelvis. Alternatively, we could define a ROI with
320 respect to the pelvis and apply it to all test conditions. However, due to the difference in seat

321 pan angle, a ROI with its axis perpendicular to the seat pan surface in the Reference condition
322 will no longer be perpendicular in the Shear condition. As we were interested in the region
323 between the IT and the seat, we preferred the first method for defining ROIs. Brienza et al.
324 (2018) used an ROI with a rectangular section, which was defined based on the specific
325 geometric characteristics of each IT for each participant in each condition. In two more recent
326 studies by Sonenblum (2018, 2020), an oblique plane of 50 mm long parallel to the IT was used
327 to define the ROI. Al-Dirini et al. (2015) also quantified the deformation of the gluteal soft tissues
328 during sitting. They estimated tissue thickness under some landmarks directly from raw MRI
329 images without 3D reconstructions. However, as identifying anatomical landmarks from MRI
330 images is not easy, results may be operator dependent.

331 Concerning the Unloaded condition (also called 'non-weight bearing'), participants here
332 were instructed to maintain a desired sitting posture in a reclined position with the help of upper
333 arm, knee, and foot supports (Figure 2), similar to the approach used in Al-Dirini et al. (2015).
334 Compared to the unloaded conditions proposed by Sonenblum et al. (2015) and Brienza et al.,
335 (2018), our Unloaded configuration had an advantage in that the buttocks and thighs were fully
336 unsupported with a position close to a normal sitting. Sonenblum et al. (2015) cut a hole on the
337 seat pan and only the region beneath the IT was unsupported. Brienza et al. (2018) adopted a
338 lying supine position with the thighs oriented vertically. Effects of gravity on soft tissues were
339 better considered in our Unloaded position. However, when looking at the pelvis femur angle
340 from the 3D reconstructions (Figure S1 in Supplemental Materials), it is much smaller in the
341 Unloaded condition than in the three seated ones, though we controlled the back thigh angle
342 close to the Reference condition. One reason could be that loading from the seat makes the
343 pelvis rotate posteriorly, as already observed by Keegan (1953) from X-ray images in 1950s.

344 In terms of soft tissue thicknesses and their composition under the IT, results from the
345 present study are comparable to past studies. For an upright sitting position corresponding to
346 wheelchair use, Sonenblum et al. (2015) observed, from 4 able-bodied and 3 individuals with

347 spinal cord injury, mean values of 21 and 14 mm, respectively, for fat and the GM in the
348 Unloaded condition and 14 and 1 mm in the Foam condition in the 10 mm cylindrical ROI. No
349 GM was observed in the 10 mm ROI except for one able-bodied participant. The mean bulk
350 tissue thicknesses in the 10 mm region were about 35 and 15 mm for the Unloaded and Foam
351 conditions if tissues other than fat and the GM muscle are neglected. We found 46 and 14.5 mm
352 in the 10 mm cylindrical ROI for Unloaded and Foam condition from 4 able-bodied males, and
353 no GM was present for any of the participants. In their study comparing three wheelchair
354 cushions across 4 full-time wheelchair users, Sonenblum et al. (2018) found that the bulk tissue
355 thickness in an oblique plane of 50 mm ROI under the ischium varied from 8 to 25mm
356 depending on participant and cushion, with a reduction of bulk tissue thickness up to 60%. For
357 the Foam condition in the present study, it varied from 15.5 to 21 mm in the 50 mm cylindrical
358 ROI with a thickness reduction from 54.8 to 69.6%. In a more recent study with 35 participants,
359 Sonenblum et al. (2020) found results comparable to their previously published pilot studies. In
360 addition, they observed that wheelchair users had thinner tissue under the ischium than did
361 able-bodied individuals.

362 Our results confirm the findings by several researchers (Sonenblum et al., 2015, 2018,
363 2020; Brienza et al., 2018) that the tissues beneath their ITs are composed predominantly of fat
364 and connective tissue in a seated position. This outcome suggests that sitting on soft or hard
365 surfaces displaces the GM laterally and posteriorly away from the IT. In a seated position, the
366 loading on the body contributes to the displacement of the GM muscle from the IT. This was
367 clearly observed for Participant 1, who had a percentage the GM muscle of 55.1% in the 50mm
368 ROI for the Unloaded condition (Table 3). Once seated, the GM percentages reduced to 10.2,
369 2.1, and 5.3% respectively in the Reference, Foam, and Shear condition (Table 4). For the two
370 narrower ROIs (20 and 10mm) beneath the IT, no presence of the GM was observed for any of
371 the four participants in any of the three seated conditions. In the work by Al-Dirini et al. (2017),
372 participants were scanned in a semi-recumbent posture using a 'tunnel' MRI system. It seemed

373 that these authors did not observe the absence of the GM muscle under the IT event for the
374 weight bearing condition, probably due to a difference in posture. The ischial point closest to the
375 contact surface was likely located more posteriorly than the more upright sitting postures
376 studied here.

377 4.3 Implications for assessing seating discomfort and injury risk

378 As explained above, three seating conditions were defined based on the findings from our
379 previous studies using a reconfigurable experimental seat (Wang et al., 2018, Wang et al.,
380 2019a). We observed that the Reference condition with a seat pan angle (A_SP) of 7° was
381 preferred for the backrest inclination tested in the present work, compared to the Shear
382 configuration with A_SP equal to 0°. An analysis of perceived seating discomfort ratings (Wang
383 et al., 2018) confirmed that the preferred seating condition (Reference) had a lower discomfort
384 rating than the seating condition with a horizontal seat pan (Shear). One explanation could be
385 that the shear force on the seat pan was reduced. The Foam configuration was the same as the
386 Reference in terms of seat pan and back angles, except that 50 mm thick foam was added.
387 Compared to the Reference, the Foam condition should have created a more uniform pressure
388 distribution and a smaller pressure under the ITs. Though we did not ask the participants to rate
389 the three seating configurations here, we can reasonably assume that the Foam condition was
390 the least uncomfortable, followed by Reference and Shear. In addition to the reduction of soft
391 tissue deformation by decreasing contact pressure, the current results seem to support that
392 reducing shear on the seat pan surface decreases soft tissue deformation under the IT.
393 Lowering soft tissue deformation can certainly reduce pressure injury risk, as sustained
394 deformations of soft tissues due to mechanical loading are the cause of initial cell death and
395 tissue damage that ultimately may result in pressure injuries (Gefen et al., 2021). Our findings
396 support the idea of using soft tissue deformation as an objective measure for assessing seating
397 discomfort and injury risk, as this measure could account for the effects of both contact pressure

398 and shear. It could be useful when a finite element human model is used for assessing seating
399 discomfort and risk based on soft tissue deformation. Future work is needed, though, to
400 establish criteria based on soft tissue deformation for discomfort and injury assessment.

401 4.4 Implications for human body modeling

402 The present work was mainly motivated by the need for data to validate finite element human
403 body models for assessing seating discomfort. As already pointed out by Sonenblum et al.
404 (2015, 2018), finite element models of the buttocks, used to evaluate wheelchair cushions and
405 pressure ulcer risk, often depict gluteus maximus coverage under the ischium as more than
406 50%. From our recent review on the finite element models of the thigh-buttock complex
407 (Savonnet et al., 2018), none of the models used in the 27 selected papers explicitly considered
408 the GM muscle sliding around the ITs. As peak pressure and shear are most likely located
409 around the ITs, more realistic modeling in this region is needed that considers muscle sliding.

410 4.5 Limitations

411 We would like to point out several limitations in the current work. As a case study, only four
412 healthy males participated in the experiment. With such a limited number of participants, the
413 findings observed in the present study only give an indication for future studies. As individual
414 characteristics such as soft tissue composition affect deformation, results are unlikely to
415 generalize to people with different body characteristics. In addition, only one foam type was
416 studied, and thus the effects of cushion characteristics should be investigated in the future.
417 Another limitation is related to the MRI imaging system. With the size of scanning window being
418 limited, we used two acquisition sequences to cover the buttock and major part of the thigh, and
419 each sequence lasted about eight minutes. During the two sequences, we asked participants to
420 do their best to keep the same sitting position. Small postural change during one sequence and
421 between two sequences was unavoidable, making it difficult to merge data of two acquisitions.
422 Lastly, this study considered only static sitting with arms crossed and not externally supported.

423 Typically, sitting can be dynamic while doing sedentary tasks. Results could be substantially
424 different if tasks are considered. Moreover, usually, arms are partially or fully supported by the
425 table or armrests and a different trunk posture may also be adopted. This may lead a different
426 loading on the buttocks and thighs. Effects of different sitting postures need to also be studied in
427 the future.

428 5 References

- 429 Al-Dirini, R.M.A., Reed, M.P., Hu J., Thewlis, D. (2015). Deformation of the gluteal soft tissues
430 during sitting. *Clinical Biomechanics* 30: 662–668
- 431 Al-Dirini, R. M. A., Nisyrios, J., Reed, M.A. & Thewlis, D. (2017). Quantifying the in Vivo Quasi-
432 Static Response to Loading of Sub-Dermal Tissues in the Human Buttock Using
433 Magnetic Resonance Imaging. *Clinical Biomechanics* 50; 70-77.
434 <https://doi.org/10.1016/j.clinbiomech.2017.09.017>
- 435 Beurier, G., Cardoso, M., Wang, X. (2017). A new multi-adjustable experimental seat for
436 investigating biomechanical factors of sitting discomfort. SAE Technical Paper 2017-01-
437 1393, 2017, doi:10.4271/2017-01-1393/
- 438 Brienza, D., Valley, J., Karg, P., Akins, J., Gefen, A. (2018). An MRI Investigation of the Effects
439 of User Anatomy and Wheelchair Cushion Type on Tissue Deformation. *Journal of*
440 *Tissue Viability*, 27, 42 53. <https://doi.org/10.1016/j.jtv.2017.04.001>.
- 441 Call, E., Hetzel, T., McLean, C., Burton, J. N., Oberg, C. (2017). Off Loading Wheelchair
442 Cushion Provides Best Case Reduction in Tissue Deformation as Indicated by MRI.
443 *Journal of Tissue Viability* 26, n° 3: 172-79. <https://doi.org/10.1016/j.jtv.2017.05.002>.
- 444 De Looze, M. P., Kuijt-Evers, L. F. M., Van Dieën, J. (2003). Sitting comfort and discomfort and
445 the relationships with objective measures. *Ergonomics*. 46: 985–997

446 Gefen, A., Brienza, D. M., Cuddigan, J., Haesler, E., Kottner, J. (2021). Our contemporary
447 understanding of the aetiology of pressure ulcers/pressure injuries. *Int. Wound J.*, 1-13,
448 DOI: 10.1111/iwj.13667

449 Goossens, R. H., Zegers, R., Hoek van Dijke, G. A., Snijders, C. J. (1994). Influence of shear on
450 skin oxygen tension. *Clin Physiol.* 14(1):111-8.

451 Hiemstra-van Mastrigt, S., Groenesteijn, L., Vink, P., Kuijt-Evers, L. F. M. (2017). Predicting
452 passenger seat comfort and discomfort on the basis of human, context and seat
453 characteristics: a literature review. *Ergonomics.* 60:889–911

454 Keegan, J. J., (1953). Alterations of the lumbar curve related to posture and seating. *J Bone
455 Joint Surg Am* 35 A(3): 589–603.

456 Olesen, C. G., De Zee, M., Rasmussen, J. (2010). Missing links in pressure ulcer research - An
457 interdisciplinary overview. *J Appl Physiol.* 108:1458–1464.

458 Rasmussen, J., Torholm, S., & de Zee, M. (2009). Computational analysis of the influence of
459 seat pan inclination and friction on muscle activity and spinal joint forces. *International
460 Journal of Industrial Ergonomics* 39: 52–57

461 Savonnet, L., Wang, X., & Duprey, S. (2018). Finite element models of the thigh-buttock
462 complex for assessing static sitting discomfort and pressure sore risk: a literature review.
463 *Computer Methods in Biomechanics and Biomedical Engineering* 21 (4): 379 88.
464 <https://doi.org/10.1080/10255842.2018.1466117>

465 Savonnet, L. (2018). Development of a customizable digital tool for assessing aircraft passenger
466 discomfort and fatigue. PhD thesis, Université de Lyon, 2018. [https://tel.archives-
467 ouvertes.fr/tel-01838797](https://tel.archives-ouvertes.fr/tel-01838797)

468 Sonenblum, S., E., Sprigle, S. H., Cathcart, J. M., Winder, R., J. (2015). 3D Anatomy and
469 Deformation of the Seated Buttocks. *Journal of Tissue Viability* 24 (2), 51-61.
470 <https://doi.org/10.1016/j.jtv.2015.03.003>.

471 Sonenblum, S. E., Ma, J., Sprigle, S. H., Hetzel, T. R., Cathcart, J. M. (2018). Measuring the
472 Impact of Cushion Design on Buttocks Tissue Deformation: An MRI Approach. *Journal*
473 *of Tissue Viability* 27, 162-172. <https://doi.org/10.1016/j.jtv.2018.04.001>.

474 Sonenblum, S. E., Seol, D., Sprigle, S. H., Cathcart, J. M. (2020). Seated buttocks anatomy and
475 its impact on biomechanical risk. *Journal of Tissue Viability* 29, 69-75.
476 <https://doi.org/10.1016/j.jtv.2020.01.004>

477 Theodorakos, I., Savonnet, L., Beurier, G., Wang, X. (2018). Can computationally predicted
478 internal loads be used to assess sitting discomfort? Preliminary results. In *Proceedings*
479 *of the 20th Congress of the International Ergonomics Association (IEA 2018)*, Edited by
480 Sebastiano Bagnara, Riccardo Tartaglia, Sara Albolino, Thomas Alexander, and Yushi
481 Fujita, 447-456. *Advances in Intelligent Systems and Computing*. Springer International
482 Publishing, 2019

483 Zhang, L., Helander, M. G. and Drury, C. G. (1996). Identifying factors of comfort and discomfort
484 in sitting, *Human Factors*, 38, 377-389

485 Wang, X., Cardoso, M., Beurier, G. (2018). Effects of seat parameters and sitters'
486 anthropometric dimensions on seat profile and optimal compressed seat pan surface.
487 *Applied Ergonomics* 73, 13–21

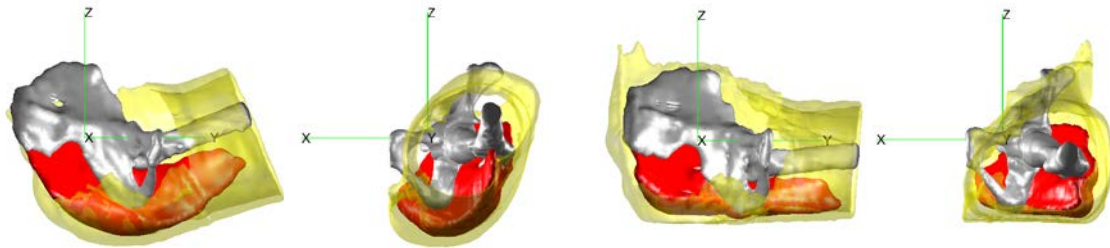
488 Wang, X., Cardoso, M., Theodorakos, I., Beurier, G. (2019a). Seat/occupant contact forces and
489 their relationship with perceived discomfort for economy class airplane seats.
490 *Ergonomics*, 62(7):891-902. doi: 10.1080/00140139.2019.1600050

491 Wang X., Savonnet L., Theodorakos I., Beurier G., Duprey S.(2019b). Biomechanical human
492 models for seating discomfort assessment. *DHM and posturography*, Editors S.
493 Scataglini and G. Paul. Academic Press, 643-659. [https://doi.org/10.1016/B978-0-12-](https://doi.org/10.1016/B978-0-12-816713-7.00049-0)
494 [816713-7.00049-0](https://doi.org/10.1016/B978-0-12-816713-7.00049-0)

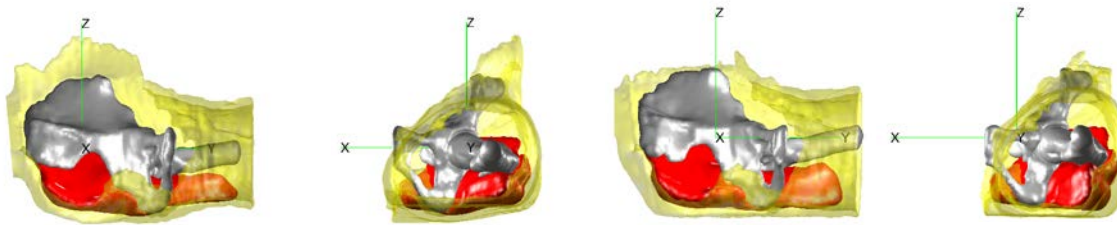
495 Zemp, R., Taylor, W.R., Lorenzetti, S., (2015). Are pressure measurements effective in the
496 assessment of office chair comfort/discomfort? A review. *Applied Ergonomics*; 48:273-82

498 **Supplemental materials**

499



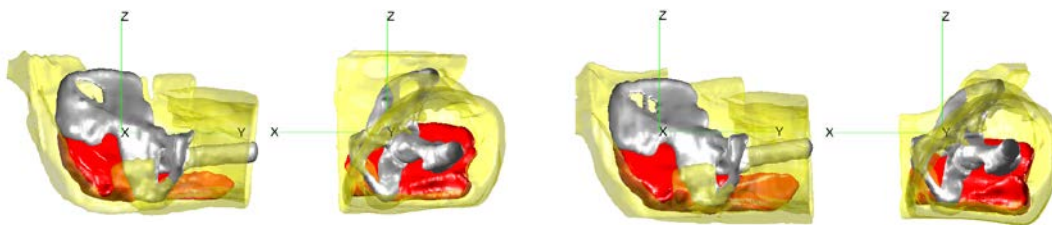
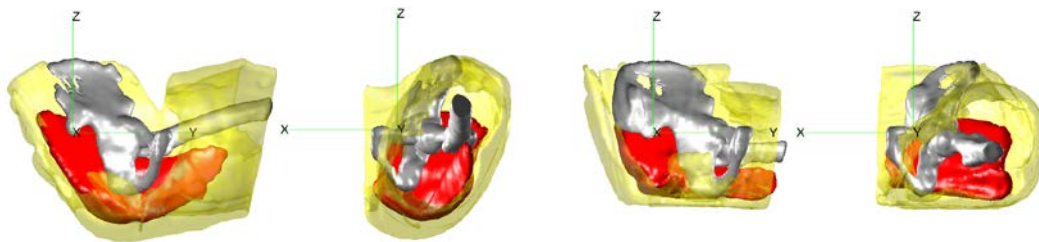
Reference



Shear

500

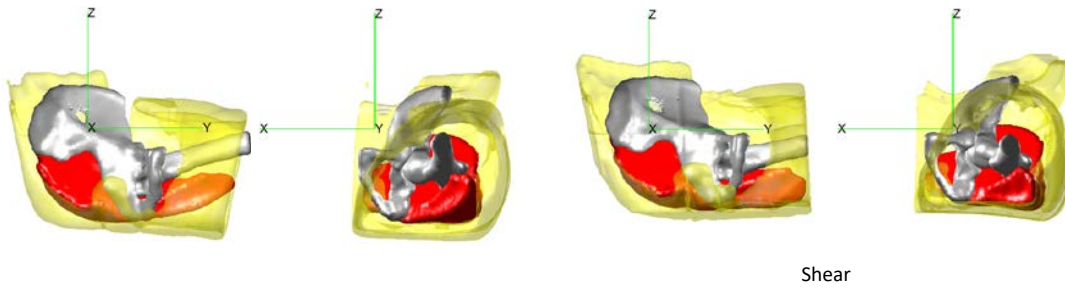
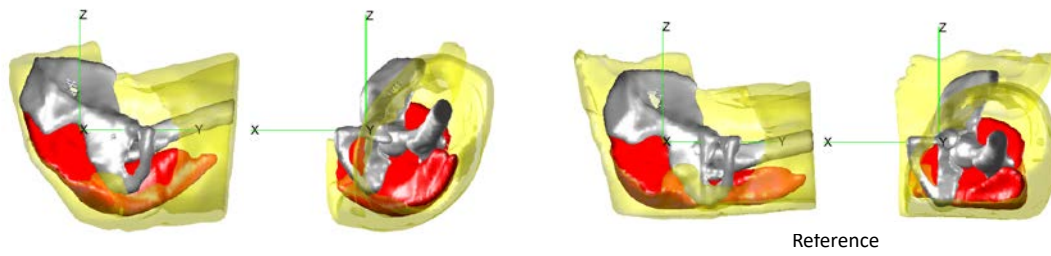
501



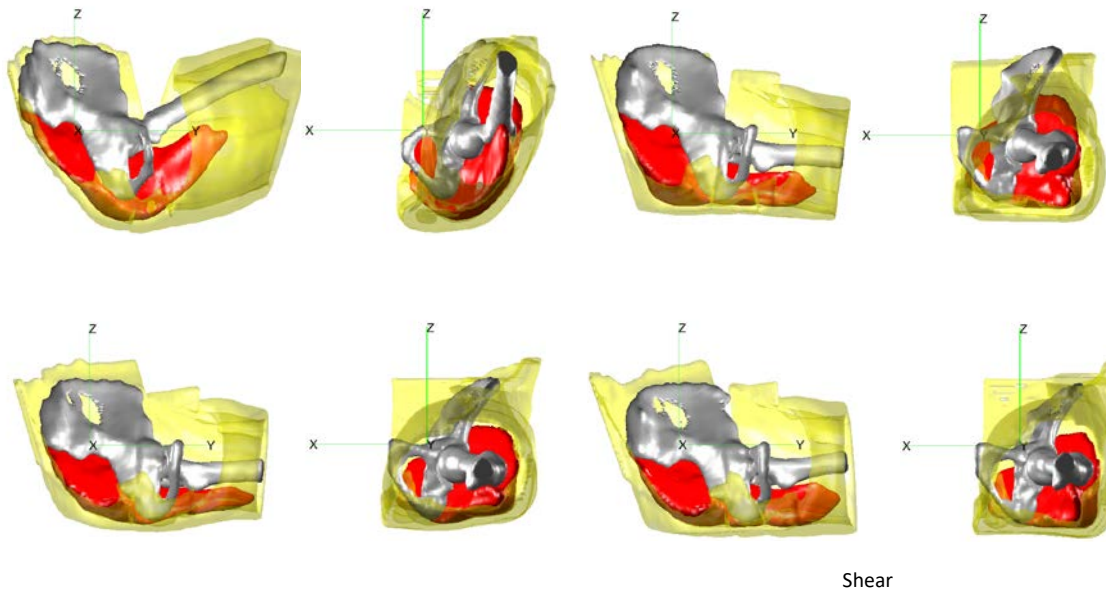
Shear

502

503

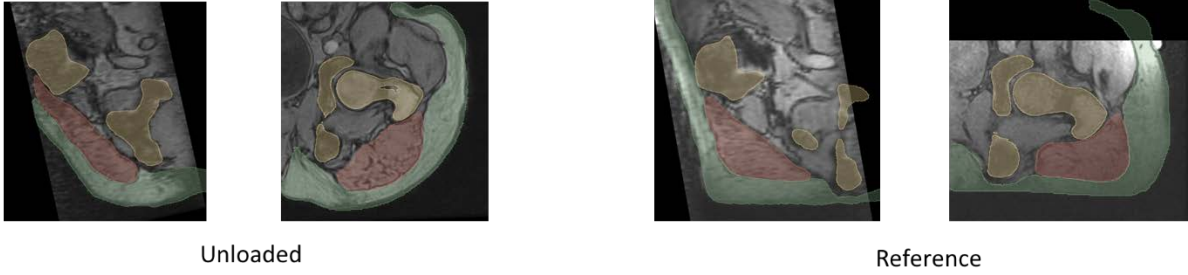


504
505



506
507
508
509
510
511
512
513

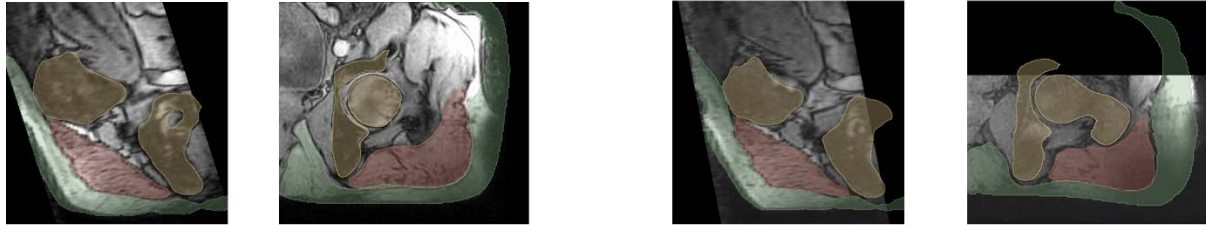
Figure S1: Reconstructed 3D representations of the pelvis, femur, GM, and fat in a seat coordinate system with the x-y plane parallel to and z perpendicular to the seat surface for the four participants. For the Unloaded condition, which had no seat pan, the 3D reconstructions are transformed so that its pelvis is aligned with that of the reference configuration.



Unloaded

Reference

Subject 3



Foam

Shear

519

520



Unloaded

Reference

Subject 4



Foam

Shear

521

522 **Figure S2: MRI Slices of the IT in the frontal and sagittal planes with segmentation (yellow: pelvis, green: fat,**
 523 **red: muscle) for the four participants. The frontal plane is perpendicular to the seat pan surface. For the**
 524 **Unloaded condition which had no seat pan, a rigid transformation is applied so that its pelvis is aligned with**
 525 **that of the Reference configuration.**

526

527